



ELSEVIER

Applied Surface Science 188 (2002) 29–35

applied
surface science

www.elsevier.com/locate/apsusc

Characterisation of Y_2O_3 thin films deposited by laser ablation on MgO: why a biaxial epitaxy

R.J. Gaboriaud*, F. Pailloux, F. Paumier

Laboratoire de Métallurgie Physique, Université de Poitiers, SP2MI, UMR 6630,
CNRS, BP 30179, 86962 Chasseneuil, Futuroscope, France

Abstract

Yttrium oxide, Y_2O_3 , thin films are deposited in situ at 700 °C by laser ablation on MgO substrate. Orientation relationships are studied by means of asymmetric X-ray diffraction and HRTEM investigations. A particular attention is paid to the growth of the (1 0 0) orientation of the oxide which seems to be strongly related to the oxygen partial pressure in the deposition chamber. An explanation in terms of a particular dislocation configuration is proposed. This configuration is linked to the oxygen partial pressure through the atom mobility in the thin oxide film. © 2002 Elsevier Science B.V. All rights reserved.

Keywords: Heteroepitaxy; Stress; Dislocations; Thin films; Oxides; Y_2O_3

1. Introduction

Significant research interest in the growth and characterisation of Y_2O_3 films has attracted much attention over the last few years because of several relevant physical properties and technical applications. Y_2O_3 is an important material for such optical application as phosphor or laser waveguide because of its ability to be a host material for rare earth atoms as europium or thulium [1–3].

Furthermore, Y_2O_3 is a promising material for electronic application as part of metal oxide–semiconductor (MOS) heterostructure used in the MOS transistor [4]. Owing to its high chemical stability up to 2325 °C, this oxide is also widely used for high temperature corrosion protection [5].

Y_2O_3 is usually deposited by RF magnetron sputtering [6], electron beam evaporation [7,8], reactive

ionised cluster beam [9,10], molecular beam epitaxy [11] and laser ablation [2–4,12,13].

Recent works are devoted to the epitaxial deposition of Y_2O_3 on a variety of single crystalline substrate among which Si [2,10,14,15], $LaAlO_3$ [12], YSZ [3,11] and MgO [3,16,17].

This work is focused on the study of the epitaxial relationships between the thin oxide film and the substrate. A particular attention is paid on the influence of the oxygen partial pressure, $P(O_2)$, on the crystalline growth direction of the film.

2. Experiments

Thin film, 300 nm thick, of Y_2O_3 has been deposited in situ at 700 °C by laser ablation of a stoichiometric Y_2O_3 target on a single crystalline (0 0 1) MgO substrate using a Nd–YAG laser with a frequency of 5 Hz and a pulse duration of 5 ns. The in situ growth of the film was achieved under different oxygen partial pressure $P(O_2)$ in the range 10^{-6} –0.5 mbar.

* Corresponding author. Tel.: +33-05-49-49-66-62;
fax: +33-05-49-49-66-92.
E-mail address: roly.gaboriaud@univ-poitiers.fr (R.J. Gaboriaud).

The epitaxial relationships between the film and the substrate were studied by asymmetric X-ray diffraction with a four-circles Siefert goniometer. Nanostructure of the film is investigated by high-resolution transmission electron microscopy (HRTEM) with a 300 kV JEOL 3010 microscope.

3. Experimental results

Thin films of Y_2O_3 were deposited on (001) MgO substrates at 700 °C under vacuum and different $P(O_2)$. The influence of the substrate and $P(O_2)$ are described in details elsewhere. This work is focused on the epitaxial relationships between the oxide film and the MgO substrate when the $P(O_2)$ which is in the ablation chamber during the deposition is increased.

3.1. Orientation relationships: X-ray investigations

The crystalline orientation of the thin film of Y_2O_3 were determined from θ - 2θ diagram which exhibits an intense (2 2 2) Y_2O_3 peak when deposition is carried out under vacuum or very low $P(O_2)$ and two peaks (2 2 2) and (4 0 0) Y_2O_3 when this $P(O_2)$ increases as it is the case at 700 °C under an oxygen pressure of 0.5 mbar.

The epitaxial relationships and the determination of the growth directions for each in-plane orientations deduced from the θ - 2θ diagram are performed by ϕ -scan X-ray experiments. The ϕ -scan results give the variants which are described in Fig. 1(a) and (b).

3.2. Epitaxial relationships: HRTEM investigations

HRTEM investigations were performed on cross-section samples of the thin film. A general view micrograph shows evidence of a columnar structure. Fig. 2 shows both (2 2 2) and (4 0 0) variants, in agreement with the X-ray measurements. White lines are the (2 2 2) plane of yttrium atoms sandwiched between two planes of oxygens. Owing to the fact that the appearance of the (4 0 0) variant seems to be strongly related to the increase of the $P(O_2)$ during the deposition process, a particular attention is paid to this variant in the following.

4. Discussion

When the deposition is realised under vacuum or very low $P(O_2)$, Y_2O_3 thin film growing process exhibits a unique heteroepitaxy (2 2 2) direction with four different in-plane orientations. When the $P(O_2)$ increases, a second variant appears, the (4 0 0) with a unique in-plane orientation corresponding to the cube (Y_2O_3) on cube (MgO) epitaxy, Fig. 1(b).

Furthermore, as $P(O_2)$ increases, the (4 0 0) orientation can become dominant. Therefore, a question arises: why a biaxial epitaxy with the appearance of a variant (4 0 0) which seems to be strongly related to the increase of $P(O_2)$? In order to get some indications for the comprehension of these phenomena, some crystallographic details must be developed. MgO is a rocksalt structure with a lattice parameter of 0.421 nm.

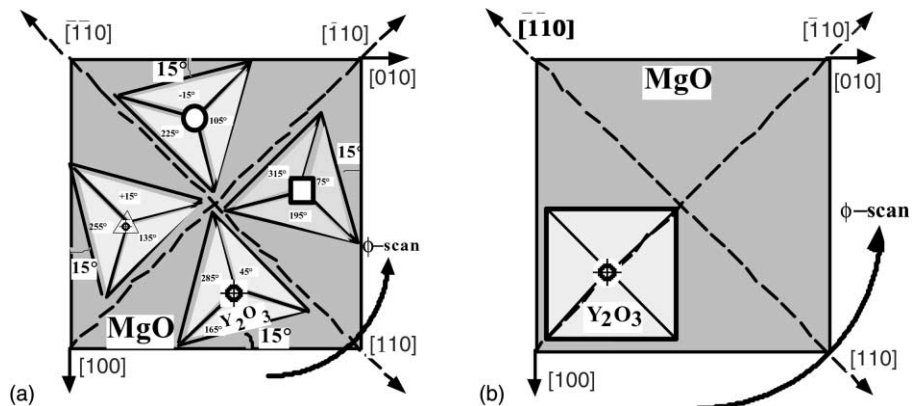


Fig. 1. Orientation relationship between the thin film of Y_2O_3 deduced from the X-ray ϕ -scan experiments: the (2 2 2) orientation with four in-plane variants (a); the (4 0 0) orientation (b).

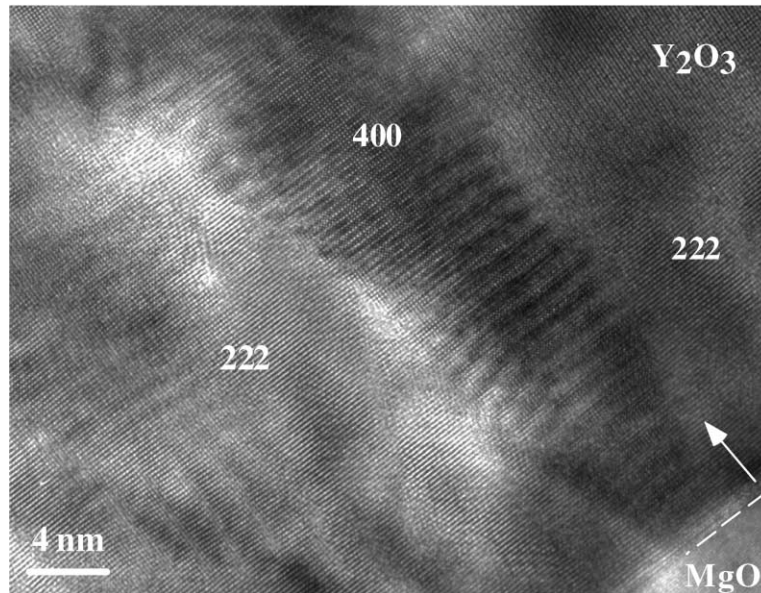


Fig. 2. HRTEM picture of a cross-section of the thin Y_2O_3 film. The (2 2 2) and (4 0 0) grains are shown together with the MgO substrate. The dashed line is the interface. The white arrow is the growth direction.

Y_2O_3 is assimilated to the cubic rare earth oxide (yttrium is not a rare earth). The structure which is cubic is called cubic-C or bixbyite, this latter is the mineral to which corresponds this structure. The unit cell contains 80 atoms [18,19]. The lattice parameter is 1.0604 nm. It is worth noting that this structure is similar to the fluorite structure (CaF_2 , UO_2 , ZrO_2 , and CeO_2), where 25% of the fluorite anions would have been removed. The Y_2O_3 structure exhibits an ordered network of oxygen structural vacancies which means that an oxygen atom on this structural site must be considered as an interstitial. Those unoccupied oxygen sites form non-intersecting string along the four $\langle 1\ 1\ 1 \rangle$ directions of the unit cell. Consequently, this structure gives several possible epitaxial orientations which can be explained in terms of near coincidence site lattice. Furthermore, those strings without oxygen provide relatively unimpeded pathways for the migration of oxygen through the material and should play an important role in the diffusional process which take place as the deposition proceeds. A consequence of this particular structure of the (2 2 2) anion planes of this oxide is a low (2 2 2) surface free energy. The (2 2 2) planes of both fluorite and bixbyite are the cleavage planes of those neighbouring structures.

4.1. The (4 0 0) variant of Y_2O_3

Generally, Y_2O_3 grows with its (2 2 2) plane on the surface plane of the substrate whatever the substrates, crystalline or amorphous, are. Owing to the fact that the (1 1 1) surface of the films has the lowest surface free energy [3,4], the nucleation of grain with (1 1 1) texture orientation is energetically much more favourable even on amorphous substrates as native SiO_2 oxide layer on Si or on fused silica [4,10,14,15]. The preferential (1 1 1) orientation changes to a mixture of (1 1 1) and (1 0 0) as the oxygen pressure is increased.

Several explanations of this phenomena have been recently suggested: the change in the film orientation should be associated to the increase of outgrowths density on the film surface due to the $P(\text{O}_2)$ increase [2]; the shift of the diffraction peaks from (2 2 2) to (4 0 0) orientation with increasing O_2 gas pressure might be due to a change in oxygen vacancy concentration and the related increase in the mobility of atoms which is of prime importance through diffusional process-induced relaxation of the microstructure during growth process [4]. This last explanation seems to be particularly interesting but should be

linked to some microstructural modification which could explain why the increase of $P(\text{O}_2)$ is beneficial to the growth of Y_2O_3 film along the (1 0 0) direction.

4.2. Crystalline defects in Y_2O_3 thin film

Owing to the arguments discussed above, it is important to study, in some detail, what are the crystalline defects which could play a major role in terms of diffusional process and the consequence on the internal free energy of a (1 0 0) crystal of Y_2O_3 .

Obviously, the surface free energy of the Y_2O_3 (1 0 0) surface is larger than the (1 1 1) surface. If the preferred orientation of Y_2O_3 film is determined by the minimisation of the overall energy including the surface free energy and the internal strain energy, it should be predicted that the crystalline defect microstructure, which built up as the growth proceeds, should be particularly relevant as a relaxation process and could be, therefore, the driving force toward the (1 0 0) grain growth.

The crystalline structure of Y_2O_3 exhibits 80 atoms per unit cell and the dislocation structures are rather complicated [20]. The shortest Burgers vector of a perfect dislocation is $\mathbf{b}_1 = \frac{1}{2}a\langle 1\ 1\ 1 \rangle$ which is 0.9 nm long. The other possible vectors are: $\mathbf{b}_2 = a\langle 1\ 0\ 0 \rangle$ (1.06 nm) and $\mathbf{b}_3 = a\langle 1\ 1\ 0 \rangle$ (1.5 nm). Curiously, the vector \mathbf{b}_3 which is the longest is responsible for the easy glide system of dislocations which takes place

in the (0 0 1) plane. It is an important point for the following.

This long Burgers vector play a major role because the related dislocations are in fact dissociated into two partials dislocations with $\mathbf{b}_p = \frac{1}{2}a\langle 1\ 1\ 0 \rangle$ in the (0 0 1) plane. The (0 0 1) plane stack of the Y_2O_3 structure is described by eight planes, four anion planes and four cation planes. The shear corresponding to $\mathbf{b}_p = \frac{1}{4}a\langle 1\ 1\ 0 \rangle$ mentioned above disturbs only the fourth plane–plane interactions as depicted in Fig. 3. Obviously, the corresponding stacking fault should have a low stacking fault energy. This point has been developed elsewhere in the past [21].

It is worth noting that this low stacking fault energy shear is the perfect Burgers vector of the fluorite structure [20]. Furthermore, the figure shows that exactly the same stacking fault can be obtained by the removal of four successive (0 0 1) planes. This leads to the so-called climb dissociation of dislocation as shown in Fig. 4. In this configuration, the stacking fault is in the climb plane and the climb motion of the partial dislocations involves diffusional process which can take place between the partials only.

Obviously, a climb dissociated dislocation microstructure with the extra planes normal to the interface with the substrate seems to be a particularly interesting clue in the interpretation of the (1 0 0) Y_2O_3 grain growth. First, because these extra planes orientations are of prime importance for the relaxation

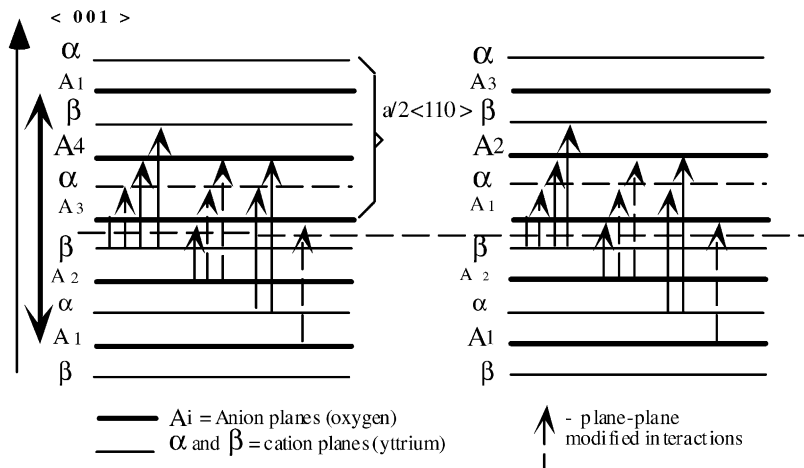


Fig. 3. Stack of the (1 0 0) planes of the bixbyite structure of Y_2O_3 . The horizontal dashed line indicates the stacking fault plane induced by the shear $\frac{1}{4}a\langle 1\ 1\ 0 \rangle$. The dashed arrow are the plane–plane interactions which are modified by the shear.

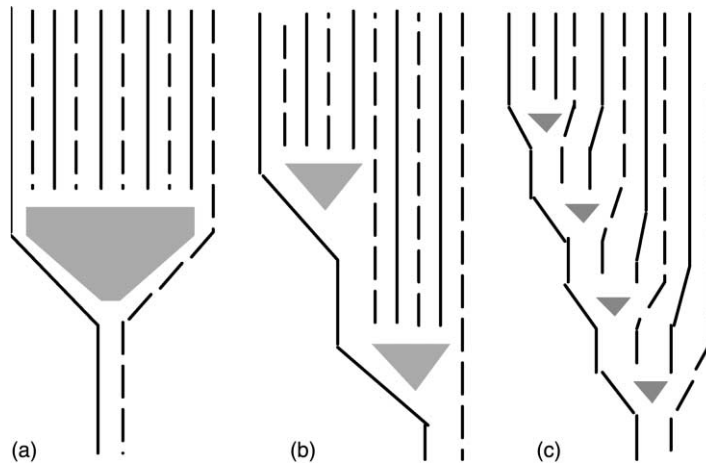


Fig. 4. Scheme of the climb dissociation process of dislocations: (a) perfect dislocation; (b) two partial; (c) four partial. Stacking fault plane is the climb plane.

phenomenon as the thin film grows and, secondly, because this dislocation configuration can adapt itself to the internal stress by a diffusional process which is directly linked to the oxygen partial pressure through the oxygen vacancy or interstitial or by anti-Frenkel pairs concentration.

From those structural arguments which are essentially due to the Y_2O_3 crystalline structure specificity, it is suggested that the microstructural configuration of dislocations plays a major role in the appearance of the (1 0 0) variant in the Y_2O_3 thin film growth.

4.3. HRTEM investigations of the (1 0 0) variant of Y_2O_3 thin films

A particular attention has been paid to the HRTEM investigations of the (1 0 0) variant on cross-section sample. Fig. 5 shows a (1 0 0) Y_2O_3 crystal with a cube on cube epitaxy on the MgO substrate. The white dots in this picture represents the yttrium atoms. In order to detect where the dislocations in this crystal are, this micrograph, Fig. 5(a), has been digitised and analysed by a phase shift map technique originally

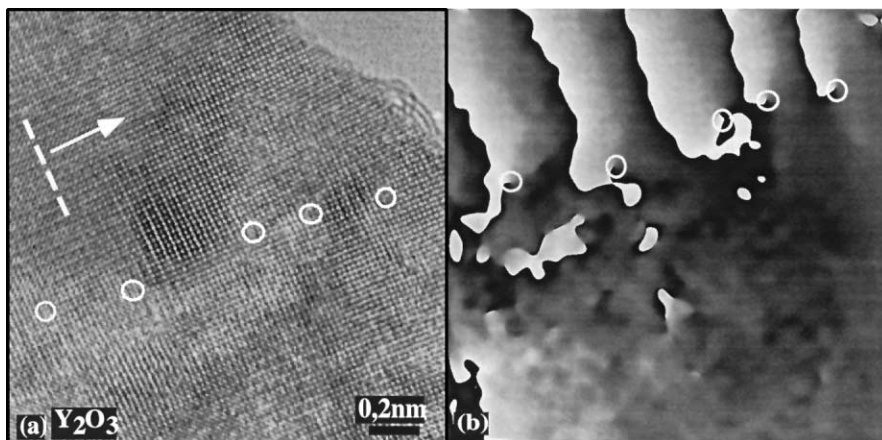


Fig. 5. (a) HRTEM picture (cross-section) of the (1 0 0) variant of the Y_2O_3 thin film; (b) analysis of (a) by the phase shift map technique (see text). White circles indicate dislocations. The dashed line is parallel to the interface with the MgO substrate. The white arrow is the growth direction.

described in detail by Hÿtch and Gandais [22]. Characteristic contrast features clearly appear (white circles) which are roughly on a line normal to the interface with the MgO substrate. A thorough examination of the HRTEM image shows that these defects are dislocations with extra half planes also normal to the interface. Furthermore, owing to the fact that the oxygen atoms are not visible, the Burgers vector of those dislocations is $\mathbf{b} = \frac{1}{4}a(1\ 0\ 0)$ (0.26 nm) and is also normal to the interface. This structure is a wall of partial dislocations with the stacking fault ribbon corresponding to their climb plane as mentioned above. Those dislocations acts as a low angle tilt boundary leading to a disorientation measured around 3–4°. This is confirmed by the relation $\theta = b/D$, where D is the average distance between the dislocations.

The observation of such tilt boundary formed with climb-induced dissociated dislocations is an important clue in the attempt to explain why the (1 0 0) Y_2O_3 variant appears. But why does this occurs, when the $P(\text{O}_2)$ increases and not under vacuum. Obviously, this is due to a diffusional process enhanced by the surrounding oxygen pressure. Owing to the defective structure of the anions network of Y_2O_3 , the diffusion of oxygen is very fast and can produce climb motion of partial edge dislocations which accommodate the internal stress energy as the deposition proceeds. The higher the $P(\text{O}_2)$ is, the higher the point defect mobility in the oxide films.

A more precise explanation may be suggested. Y_2O_3 deposited under vacuum is always under stoichiometric as shown by RBS measurements [15]. This point should produce a high disorder of the oxygen network leading to the impossibility to provide stacking fault of low energy involved in the tilt boundary mentioned above. As the $P(\text{O}_2)$ increases, the oxygen network tends to restore the stoichiometric order of the structure making highly feasible the stacking faults which are necessary to the tilt boundary formed with climb-induced partial dislocations.

5. Conclusion

Heteroepitaxy of Y_2O_3 thin oxide films deposited in situ on MgO by laser ablation has been studied. A particular attention is paid to the influence of the oxygen partial pressure on the growth crystallographic

direction of the oxide. Generally, Y_2O_3 shows a preferential growth direction which is due to the low surface free energy of the (1 1 1) planes. But, when the $P(\text{O}_2)$ is increased in the deposition chamber, a second variant with the (1 0 0) orientation appears which seems to be strongly related to the oxygen diffusivity. An explanation in terms of dislocation configuration is proposed. The specificity of the Y_2O_3 structure allows the climb dissociation of dislocations with a small Burgers vector. Furthermore, those dislocations should be highly mobile in relation with the high diffusivity of the oxygen atoms due to the external oxygen partial pressure. This explanation is supported by the HRTEM observation of low angle tilt boundary formed with such climb dissociated dislocations. This particular structure of defects can accommodate the internal stress energy and, therefore, promotes the formation and growth of the (1 0 0) variant in the Y_2O_3 thin oxide films.

References

- [1] A. Polman, J. Appl. Phys. 82 (1997) 1.
- [2] S.L. Jones, D. Kumar, R.K. Singh, P.H. Holloway, Appl. Phys. Lett. 71 (3) (1997) 404.
- [3] A. Huignard, A. Aron, P. Aschehoung, B. Viana, J. Thery, A. Laurent, J. Perriere, J. Mater. Chem. 10 (2000) 549.
- [4] S. Zhang, R. Xiao, J. Appl. Phys. 83 (7) (1998) 3842.
- [5] K. Bundschuh, M. Schÿtze, C. Mÿller, P. Creil, H. Heider, Eur. Ceram. Soc. 18 (1998) 2389.
- [6] W.M. Cranton, D.M. Spink, R. Stevens, C.B. Thomas, Thin Solid Films 226 (1993) 156.
- [7] R.N. Sharma, T. Lakshami, R.C. Rastogi, Thin Solid Films 199 (1991) 1.
- [8] A. Ichinose, A. Kikuchi, K. Tachikawa, S. Akita, Physica C 302 (1998) 51.
- [9] S.C. Choi, M.H. Cho, S.W. Wahangbo, C.N. Wang, S.B. Kang, S.J. Lee, M.Y. Lee, Appl. Phys. Lett. 71 (1997) 903.
- [10] M.H. Cho, D.H. Ko, K. Jeong, S.W. Whangbo, C.N. Wang, S.C. Choi, S.J. Cho, J. Appl. Phys. 85 (1999) 2909.
- [11] R.L. Goetler, J.P. Maria, G. Schlom, Mater. Res. Soc. Symp. Proc. 477 (1997) 333.
- [12] H.J. Gao, D. Kummar, K.G. Cho, P.H. Holloway, R.K. Singh, X.D. Fan, Y. Yan, S.J. Pennycook, Appl. Phys. Lett. 75 (1999) 2223.
- [13] M.B. Korzenski, P. Lecoeur, M. Mercey, D. Chippaux, B. Raveau, Chem. Mater. 12 (2000) 3139.
- [14] R.H. Horng, D.S. Wu, J.W. Yu, C.Y. Kung, Thin Solid Films 289 (1996) 234.
- [15] R.J. Gaboriaud, F. Pailloux, P. Guerin, F. Paumier, J. Phys. D 33 (2000) 2884.

- [16] R.J. Gaboriaud, F. Pailloux, J. Pacaud, P.O. Renault, J. Perriere, A. Huignard, *Appl. Phys. A* 71 (2000) 675.
- [17] M. Hasegawa, Y. Yoshida, M. Iwata, K. Ashizawa, Y. Takai, I. Hirabayashi, *Physica C* 336 (2000) 295.
- [18] L. Pauling, M.D. Shapell, *Z. Krist. B* 75 (1930) 128.
- [19] B.H. O'Connor, T.M. Valentine, *Acta Cryst. B* 25 (1969) 2140.
- [20] R.J. Gaboriaud, M.F. Dennaot, M. Boisson, J. Grilhe, *Phys. Stat. Sol. A* 46 (1978) 387.
- [21] R.J. Gaboriaud, M. Boisson, *J. Phys. Fr. C6-7* (1980) 171.
- [22] M.J. Hÿtch, M. Gandais, *Phil. Mag. A* 72 (1995) 19.